Fabrication of Field Effect Devices Based on YBaCuO/PrBaCuO/YBaCuO Junctions

Hiroshi Kimura and Yoichi Okabe
Research Center for Advanced Science and Technology, The University of Tokyo,
4-6-1, Komaba, Meguro-ku, Tokyo 153, Japan

Hiroshi Kamijo
Functional Device Laboratory , Fuji Electric Corporate Research and Development, Ltd. ,
2-2-1, Nagasaka Yokosuka City, 240-01 Japan

***Abstract*—In order to investigate an electric field effect in the junction, the three terminal device was fabricated. When the gate voltage of +2V (E=7×10^4 V/cm) was applied, the drain-source resistance decreased above the temperature of 100K. However, the electric field effect could not be observed below the temperature of 100K. Above the temperature of 100K, it is found that the CuO chain in PBCO behaved itself as a doped semiconductor (acceptor level = 26.5 meV).**

I. Introduction

Recently, YBa2Cu3O7-x/PrBa2Cu3O7-y/YBa2Cu3O7-x (YBCO/PBCO/YBCO) junctions have been fabricated by several authors [1]-[5]. These junctions showed typical characteristics of SNS Josephson junctions. This suggests that the order parameter was not significantly suppressed at the interface between YBCO and PBCO. One of reasons why YBCO/PBCO have a good interface is that there is not any significant interface resistance. This is because there are not any sort of oxygen dificiency / disorder at the interface since the thermal expansion of c-axis of PBCO is similar to that of YBCO [6]. On the other hand, if YBCO/PBCO/YBCO junction has an ideal SNS interface, the order parameter is not significantly decayed at its interface according to the theoretical calculation using carrier densities of YBCO and PBCO. Our goal is to control the order parameter in PBCO by changing its carrier concentration by applying an electric field. In this paper, we try to fabricate a three terminal device which have a insulating gate on PBCO on YBCO/PBCO/YBCO planar type junction to understand the electric field effect in the junction.

II. Experiments

Figure 1 shows schematic illustration of our three terminal device. Pt and SrTiO3 (STO) were chosen as a gate electrode and a gate layer respectively. STO layer on Pt (100) shows (100) orientation which is the same orientation as the substrate. Pt and STO layers were deposited on STO(100)

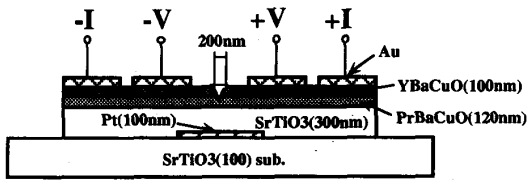

Fig. 1. Schematic illustration of three terminal device based on YBCO/PBCO/YBCO junction.

substrate by rf magnetron sputtering method. The depositions of Pt layer were carried out at a temperature of 650°C, Ar pressure of 0.5Pa and the sputtering power of 300W using a metal mask. Depositions of STO were done the temperature of 650°C, the gas pressure (Ar/O2=1) of 0.5Pa and sputtering power of 200W. YBCO and PBCO layers were deposited on STO(100)/Pt(100) layers by rf magnetron sputtering method. Detailed deposition conditions were reported previously [7]. We chose a-axis oriented YBCO/PBCO films for fabrication of devices, since the junctions using a-axis oriented YBCO/PBCO/YBCO films showed typical characteristics of the SNS junction; we thought that the order parameter is not significantly suppressed at its interface. The planar type YBCO/PBCO/YBCO junctions were fabricated on STO/ Pt layers by a focused ion beam (FIB) technique and a conventional photolithography. The detailed experimental etching method was also described previously [8]. After the fabrication of planar type junction, the STO layer was etched off by 5% HF to obtain the gate electrode of Pt. Resistivity-Temperature characteristics (R-T characteristics) and Current-Voltage characteristics (I-V characteristics) were measured by the conventional four probe method. Capacitance and tanδ were measured by the LCZ meter. Surface morphologies of films were observed by scanning electron microscope (SEM).

Manuscript received October 18, 1994

III. Results and Discussion

A. Gate Insulator

We first deposited STO film with the thickness of 300 nm on Nb-doped-STO (100) substrate. We used Nb-doped-STO substrate as lower electrode since this substrate is semiconductor. The STO film deposited on this substrate was the best film. For electrical measurement, Au electrodes were deposited on the film using a metal mask. The permittivity and tanδ at 10kHz for this film were 195 and 0.018 at room temperature respectively. At the temperature of 77K, the permittivity and tanδ were 336 and 0.015 respectively. On the other hand, the gate insulator, STO, was deposited Pt layer instead of Nb-doped-STO for device applications as shown in Fig. 1. The value of tanδ of the gate insulator was 0.12. It seems that our gate insulator on Pt layer was not crystallized completely such as the STO on Nb-doped-STO substrate. Figure 2 shows a 60-degree angle SEM photograph of the bridge which were fabricated on Pt layer. Although we could not confirm the interface between YBCO and PBCO, the STO layer could be observed distinctly. This photography indicates that the STO layer was grown uniformly and we could observe no short between upper and lower layers. The I-V characteristic of a STO layer with a thickness of 300 nm is shown in Fig. 3. In this figure, positive electrode is Pt layer. The voltage at which the leak current exceeded 1nA was +7V ($E=2.4\times10^5$V/cm) at the temperature of 64K. The breakdown voltage was increased with decreasing the temperature. When the upper electrode was changed from YBCO/PBCO double layers to Au metal, the negative breakdown voltage was decreased considerably. Although the mechanism of breakdown is not clear now, we believe that the breakdown occurred at the interface between STO and other materials.

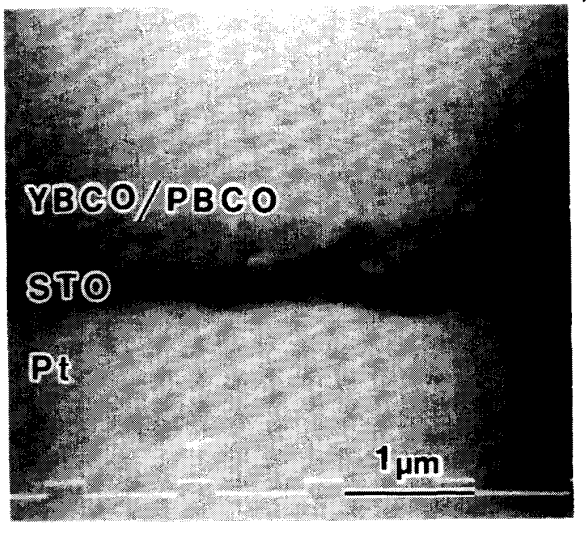

Fig. 2. 60-degree angle SEM photograph of the bridge structure.
YBCO: 100nm, PBCO: 120nm, STO 300nm , Pt:

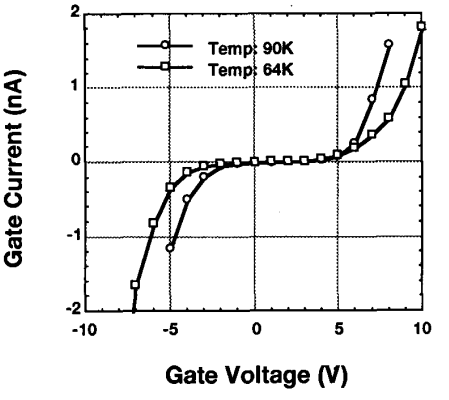

Fig. 3. Gate current-gate voltage characteristics of STO with thickness of 300nm. Positive electrode is Pt.

B. Characteristics of the three terminal device

Figure 4 (a) shows the temperature dependence of the drain-source resistance on applied gate voltage of +2V ($E=7\times10^4$ V/cm). We measured R-T characteristic with flowing the constant current of 1μA. The drain-source resistance shows the sum of two resistances. One is at the superconducting electrode. The other is the PBCO's resistance under the groove which was fabricated by FIB. The width and the depth of the groove were 0.2μm and 130nm respectively. The detail structure and characteristics of the planar type junction with the groove were reported previously [8]. Above the temperature of the critical temperature (Tc) of YBCO, the source-drain resistance was dominated by the resistance of the superconducting electrode, since the resistance under the groove is still lower than the spreading resistance of electrodes. Below Tc, the drain-source resistance was dominated by the PBCO's resistance under the groove, because the electrodes were superconducting.

When a gate voltage of +2V (leak current < 1nA) was applied to this planar type junction, the drain-source resistance was decreased above the temperature of 100K as shown in Fig. 4 (b). On the other hand, the drain-source resistance was not changed by the applied gate voltage below the temperature of 100K as shown in Fig. 4 (c).

C. Discussion

Here we discuss why the electric field effect was observed above the temperature of 100K. We consider that electrical characteristics of PBCO were changed form the variable range hopping (VRH) conduction to a semiconductor-like conduction along with temperature rise.

The resistivity dependence on temperature of the two dimensional VRH conduction is given by the following equation [9].

$$\rho = \rho_0 \exp(T_0 / T)^{1/3}.$$

where

$$T_0 = 8\alpha^2 / k_B dN(E_F).$$

kB is Boltzmann's constant, α^{-1} is the radius of the localized state wave function, d is the film thickness and $N(E_F)$ is the density of localized states. According to the theory of the VRH conduction, a density of localized state is increased with decreasing the value of T0. The temperature dependence of the resistivity of PBCO can be controlled by changing the cooling process after the deposition [8]. In our experiment, we fabricated the device using the PBCO which showed the lowest resistivity of all we could obtain, because the PBCO with the lowest resistivity, we believe, had the longest coherent length. The temperature dependence of the resistivity for PBCO film is shown in Fig. 5 in log ρ-$T^{-1/3}$ scale. The value of T0 of the film (a) was 4.1×10^3 K. The film (a) was deposited on a STO(100) substrate under the same conditions as that of device fabrication and showed a-axis orientation. When this film(a) was annealed at 300°C in flowing O2 gas, the resistivity was increased at all temperatures as shown in Fig. 5 (film (b)) and the value of T0 of the film (b) became 3.3×10^5 K. The temperature dependence of the resistivity for the film (b) showed VRH conduction at all temperatures as shown in Fig. 5. These results suggest that the PBCO in the three terminal device had more localized states than a bulk of PBCO. It is noted that the log ρ-$T^{-1/3}$ relation of the film (a) deviated from the linearly increasing above the temperature of about 100K ($100^{-1/3}$=0.215) owing to a lot of localized states.

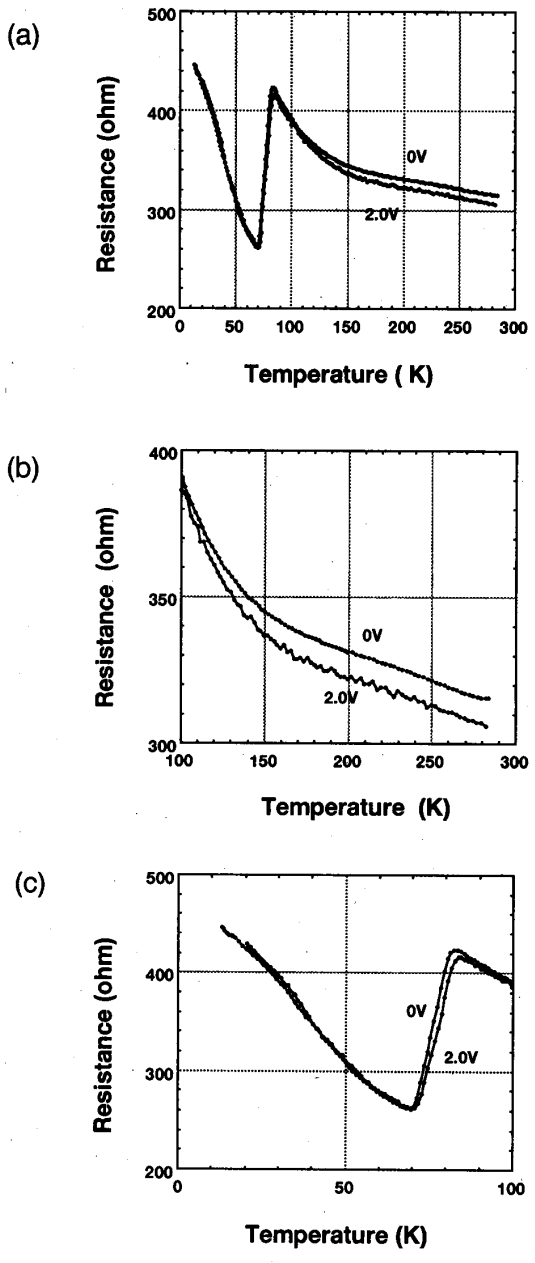

Fig. 4. R-T characteristics of the three terminal device (a) at all temperatures, (b) above 100K and (c) below 100K respectively.

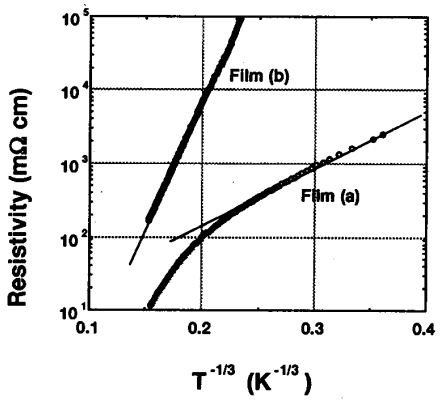

Fig. 5. Temperature dependence of the resistvity of PBCO in log ρ -$T^{-1/3}$ scale.
The device was fabricated using the film (a). The film (b) was annealed at 300 °C with flowing O2.

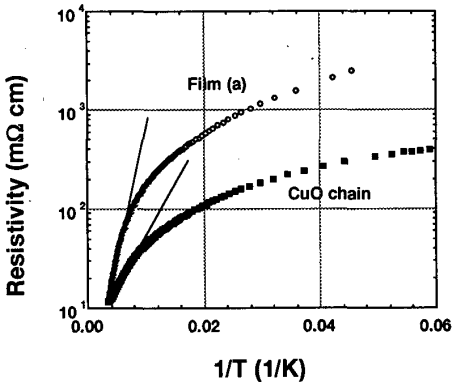

Fig. 6. Temperature dependence of the resistvity of PBCO in log ρ- 1/T scale.
The device was fabricated using the film (a). The resistivity of CuO chain was measured using (013) oriented PBCO film on STO (110) substrate.

On the other hand, the resistivity of conventional doped semiconductor is an exponential function of temperature; the resistivity is proportional to $e^{-E/kT}$. The temperature dependence of the resistivity for the film (a) is shown in Fig. 6 in log ρ-T^{-1} scale. At higher temperature of 100K (1/100=0.1), the temperature dependence of resistivity of the film (a) showed a conventional doped semiconductor-like-behavior. It was estimated from Fig. 6 that an acceptor level of a-axis oriented PBCO was 60.5 meV (EA/kB=703K). This value is slightly high to explain electrical properties of PBCO as the semiconductor at temperatures of 100-300K.

However, Y. Suzuki et al. [10] reported recently that the resistivity of PBCO was dominated by the conduction of CuO chain in PBCO. We measured the resistivity of CuO chain using (013) oriented film which was deposited under the same conditions as the film(a) on STO(110) substrate [8]. The temperature dependence of resistivity of CuO chain was also shown in Fig. 6. In this figure, it was estimated that the acceptor level of the CuO chain was 26.5meV (EA/kB=308K). This value of the acceptor level corresponded with the room temperature. These results suggest that the electric field effect in our device could be observed when the CuO chain in PBCO behaved itself as the conventional doped semiconductor. Below the temperature of 100K, the transport of the PBCO was changed from the semiconductive conduction to the VRH conduction; free holes in the PBCO were decreased with decreasing the temperature. It may be difficult to move the localized carrier by applying the gate voltage at low temperature.

IV. Summary

In conclusion, we fabricated three terminal devices to investigate the electric field effect in the YBCO/PBCO/YBCO junction. When the gate voltage of +2V was applied, the drain-source resistance was decreased above the temperature of about 100K. Below 100K, we could not observed the electric field effect in the junction. The PBCO in the present experiment was the lowest resistivity of all we could obtain and had more localized states than that of a bulk at lower temperature. We found that the CuO chain in this PBCO behaved itself as a doped semiconductor above the temperature of 100K. At lower temperature, the PBCO showed a conventional VRH conduction. We believe that the electric field effect could be observed when the barrier PBCO behaved itself as a doped semiconductor.

Acknowledgment

The authors would like to thank Mr. D. Yamaguti for the deposition of Pt, Miss M. Machidori for the SEM observation and Mr. T. Matsui, T. Suzuki, and M. Miyazaki for helpful discussions.

References

[1] C. T. Roger, A. Inam, M. S. Hegde, B. Dutta, X. D. Wu, and T. Venkatesan, " Fabrication of heteroepitaxial YBa2Cu3O7-x-PrBa2Cu3O7-x-YBa2Cu3O7-x Josephson devices grown by laser deposition," *Appl. Phys. Lett.*, vol. 55, pp. 2032-2034, 1989.

[2] J. B. Barner, C. T. Rogers, A. Inam, R. Ramesh, and S. Bersey, " All a-axis oriented YBa2Cu3O7-x-PrBa2Cu3O7-x-YBa2Cu3O7-x Josephson devices operating at 80K," *Appl. Phys. Lett.*, vol. 59, pp. 742-744, 1991.

[3] J. Gao, Yu. M. Boguslavskij, B. B. G. Klopman, D. Terpstra, R. Wijbrans, G. J. Gerritsma, and H. Rogalla, " YBa2Cu3Ox/PrBa2Cu3Ox/YBa2Cu3Ox Josephson ramp junctions, " *J. Appl. Phys.*, vol. 72, pp. 575-583, 1992.

[4] T. Hashimoto, M. Sagoi, Y. Mizutani, J. Yoshida, and K. Mizushima, " Josephson characteristics in a-axis oriented YBa2Cu3O7-δ/PrBa2Cu3O7-δ'/YBa2Cu3O7-δ junctions, " *Appl. Phys. Lett.*, vol. 60, pp. 1756-1758, 1992.

[5] E. Polturak, G. Koren, D. Cohen, E. Aharoni, G. Deutscher, " Proximity Effect in YBa2Cu3O7/Y0.6Pr0.4Ba2Cu3O7/YBa2Cu3O7 junctions, " *Phys. Rev. Lett.*, vol. 67, pp. 3038-3041, 1991.

[6] K. Char, L. Antognazza, and H. Gballe, " Study of interface in epitaxial YBa2Cu3O7-x/barrier/YBa2Cu3O7-x junctions, " *Appl. Phys. Lett.*, vol. 63, pp. 2420-2422, 1993.

[7] H. Kimura, M. Miyazaki, K. Tsuda, and Y. Okabe, " Characteristics of Josephson Junctions using the crack in YBCO Thin Film, " *IEEE Trans. Appl. Superconductivity*, vol 3, pp. 2413-2416, 1993.

[8] H. Kimura, H. Watabe, K. Mukae, and Y. Okabe, " The Electrical Properties of PrBaCuO in YBaCuO/PrBaCuO/YBaCuO Junction, " *Advances in Superconductivity VI*, T. Fujita and Y. Shiohara, Eds. Tokyo: Springer-Verlag, 1994, pp. 1067-1070.

[9] J. J. Hauser, " Electrical Structural and Optical Properties of Amorphous Carbon, " *J. Non-Crystalline Solids*, vol. 23, pp. 21-41, 1977.

[10] Y. Suzuki, J. -M. Triscone, C. B. Eom, M. R. Beasley, and T. H. Geralle, " Evidence for Long Localization Length along b Axis PrBa2Cu3O7 in a Axis YBa2Cu3O7/a, b Axis PrBa2Cu3O7 Superlattices, " *Phys. Rev. Lett.*, vol. 73, pp. 328-331, 1994.